

*inertia moment, induction motor, wavelet transformation,
backlash zone, membership function*

Marcin TOMCZYK^{[0000-0002-5383-7168]*},
Anna PLICHTA^{[0000-0001-6503-308X]**}, *Mariusz MIKULSKI*^{***}

APPLICATION OF IMAGE ANALYSIS TO THE IDENTIFICATION OF MASS INERTIA MOMENTUM IN ELECTROMECHANICAL SYSTEM WITH CHANGEABLE BACKLASH ZONE

Abstract

This paper presents a new method of identification of inertia moment of reduced masses on a shaft of an induction motor drive being a part of an electromechanical system. The study shows the results of simulations performed on the tested model of a complex electromechanical system during some changes of a backlash zone width. An analysis of wavelet scalograms of the examined signals carried out using a clustering technique was applied in the diagnostic algorithm. The correctness of the earliest fault detection has been verified during monitoring and identification of mass inertia moment for state variables describing physical quantities of a tested complex of the electromechanical system.

1. INTRODUCTION

Detection of undesirable changes of states of electromechanical processes takes the form of a sequence of intentional operations executed in assumed time using a set of machines and devices at a determined number of available resources. Faults and other destructive events can be the reasons for these changes of states (Korbicz, Kościelny & Kowalczyk, 2002).

* Electrical School No. 1 in Krakow them. Silesian Insurgents, Kamińskiego 49,
30-644 Kraków, Poland, tomczykmarcin@poczta.fm

** Cracow University of Technology, Faculty of Physics, Mathematics and Computer Science,
Institute of Computer Science, Warszawska 24, 31-155 Kraków, Poland, aplichta@pk.edu.pl

*** State University of Applied Sciences in Nowy Sącz, Institute of Technology, Zamenhofa 1a,
33-300 Nowy Sącz, Poland, mmikulski1@poczta.onet.pl

In electromechanical systems, such detection is easier due to the possibility of examining the signals simultaneously in the time and frequency, which facilitates the selection of information and, subsequently, correct interpretation of the features that assign the caught signals to different undesirable states of the system indicating the appearance of the fault (Duda, 2007; Zajac, 2009).

Recognition of images consists in detection, interpretation, and identification of the correct features in a certain set of the examined object. The process of ascribing the object to a single class is named identification, whereas the ascribing of objects to the respective classes is named classification (Looney, 1997).

There are several scientific studies on the new techniques of detection of faults in dynamic systems using time-frequency methods as well as image analysis. Among these papers, some are very recent (they were published in the last three years) and some are older. The following ones are worth mentioning:

- using the theory of waves in the identification of dynamic systems (Hasiewicz & Śliwiński, 2005; Wysocki, 2006),
- a comparative analysis of time-frequency methods in diagnostics of electric drives (Sajjad, Zaidi, Zanardelli, Aviyente & Strangas, 2007),
- analysis of the possibility of application of discrete wavelet transformation to the envelope of stator's current to the early detection of coil short circuits in induction motor indicating a fault (Wolkiewicz & Kowalski, 2015),
- sing of discrete packet wavelet analysis of signal of stator's current in the detection of faults in windings of stator's induction motor (Mathew, 2017),
- detection of rotor's cracks in induction motor using the algorithm of recognition of binary image created as a result of the transformation of the tested vector of the stator's current (Divdel, Moghaddam & Alipour, 2016),
- presentation of diagnostics of faults in three-phase induction motor using the method of extraction of features from the thermograms registered for the assumed states of working (Głowacz & Głowacz, 2017).

2. PRESENTATION OF MODEL OF THE INDUCTION MOTOR DRIVE USED IN SIMULATION TESTS OF FAULT IDENTIFICATION

The diagnostic tests have been conducted by means of a working machine in the form of a dynamic mass-absorbing-elastic element being a load to the induction motor. The nominal operating conditions of the induction motor were set, and the model has been placed in a stationary coordinate system related to the stator (model $\alpha, \beta, 0$). The gradually increasing backlash zone occurs on the rod as a result of the line's slip on the surface of the drive wheel of the working machine.

Fig.1 shows a simplified form of a diagram of the tested complex electro-mechanical system.

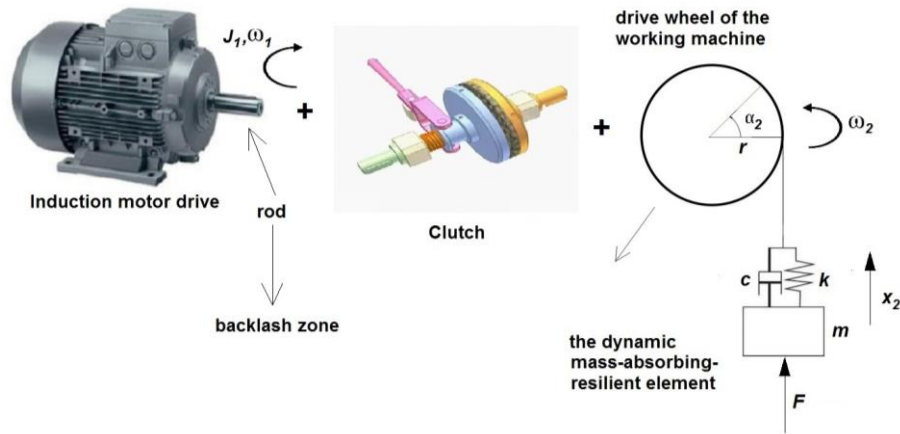


Fig. 1. Diagram of the tested complex electromechanical system – the induction motor drive is connected with the dynamic mass-absorbing-elastic element with the clutch

The following parameters of the induction motor were selected for the examination (parameters of its equivalent circuit are expressed in relative units): circuit stator relative resistance $r_s = 0.059$ [Ω], circuit rotor relative resistance $r_w = 0.048$ [Ω], relative reactance of the dispersion circuit stator $x_s = 1.92$ [Ω], relative reactance of the dispersion circuit rotor $x_w = 1.92$ [Ω], relative reactance of the dispersed circuit $x_m = 1.82$ [Ω], $w = x_s \cdot x_w - x_m \cdot x_m = 0.374$, mechanical time constant $T_m = 0.86$ [s]. All simulation tests have been conducted using MATLAB/Simulink environment.

3. DESCRIPTION OF EXECUTION OF IDENTIFICATION TESTS OF THE MASS INERTIA MOMENT IN THE ELECTROMECHANICAL SYSTEM CONTAINING FRICTION DESCRIBED BY MEANS POWER EQUATION OF OSTWALD AND DE WAELE

The tests have been carried out in four test groups, with the following four different values of apparent viscosity coefficient η_k : 0.0125 [$\text{Pa} \cdot \text{s}^{\eta_1}$], 0.025 [$\text{Pa} \cdot \text{s}^{\eta_1}$], 0.0375 [$\text{Pa} \cdot \text{s}^{\eta_1}$], and 0.05 [$\text{Pa} \cdot \text{s}^{\eta_1}$]. Each test group contained seven cases to study with different inertia moment values. The results of simulations for all the physical quantities and for every case of change of inertia moment of reduced masses and connected stiffly with the induction motor drive rotor J_1 have been written in the matrix N_1 [7,2048]. The elements of the matrix N_1 have been written for each consistency index η_k . Value of an inertia moment J_1 have been determined as the percentage in relation to its nominal value J_1 , down at value A% and up at value C%. Formal changes of inertia moment J_1 have been written in matrix K_1 in the following order: $K_1 = [\text{nominal value of the inertia moment } (J_1 = 1.16 \text{ [kg} \cdot \text{m}^2])$,

A = 2.5% ($J_1 = 1.131$ [kg·m²]), A = 5% ($J_1 = 1.102$ [kg·m²]), A = 7.5% ($J_1 = 1.073$ [kg·m²]), A = 17.5% ($J_1 = 0.957$ [kg·m²]), C = 2.5 % ($J_1 = 1.189$ [kg·m²]), C=5% ($J_1 = 1.218$ [kg·m²]).

In each of the seven cases of changes of inertia moment J_1 , simulation tests have been conducted for six backlash zone widths. The backlash zone width values have been taken in sequence from the matrix K_2 , in the following order: [0.0025, 0.00375, 0.005, 0.0075, 0.009, 0.01]. All tests have been executed for the creep index n_1 value equal 0.93.

The wavelet type and its order have been selected in such a way that the shape of the basic wavelet approximately would be adequate to the character of the transient course of the tested physical quantity obtained as a result of a simulation for the case of the smallest backlash zone width. Based on the performed tests, the following selections of wavelets have been made for individual physical variables, with decomposition level 10:

- a) linear acceleration of the induction motor drive a_1 – sym5,
- b) electromagnetic moment of the induction motor drive m_{el} – db6,
- c) angular speed of the induction motor drive rotor ω_1 – sym5,
- d) linear acceleration of a mass a_2 – db6,
- e) linear speed of a mass v_2 – sym5.

In all the conducted simulations it was assumed that the test of dynamics of the electromechanical system in backlash zone starts precisely when the expression specified in the left part of the following inequality (1) is smaller than its right part:

$$|\alpha_1 - \alpha_2| < \frac{K_{2(i)}}{r}; \quad i = 1, 2..6 \quad (1)$$

where: r – radius of the drive wheel of a working machine [m],
 $K_{2(i)}$ – value that has been taken sequentially from the K_2 matrix and corresponding to the given backlash value in mechanical connection,
 i – an index number within the K_2 matrix.

The location change of the angle α_1 for rotating masses of the induction motor drive [rad] has been calculated using the formula: $\alpha_1 = \int \omega_1 \cdot dt$, and the location change of the angle α_2 of the drive wheel of the working machine [rad], has been calculated using the formula: $\alpha_2 = \int \omega_2 \cdot dt$, where ω_1 and ω_2 stand for angular speeds. The former refers to the angular speed of rotating masses of the induction motor drive [rad/s], and the latter to the speed of the drive wheel of the working machine [rad/s].

After satisfying the condition determined by inequality described by the formula (1) the load moment of the induction motor drive is set to zero in the tested electromechanical system.

In all the conducted simulation tests it was assumed that the tested matrix N_1 would contain 2000 samples of a signal, chosen in sequence from the moment of appearance of backlash zone in the tested model of the electromechanical system; additionally, 48 samples preceding this moment would be included. Therefore, the total number of samples will amount to the value of $2^{11} = 2048$, which enables effectively to carry out a multiresolution analysis.

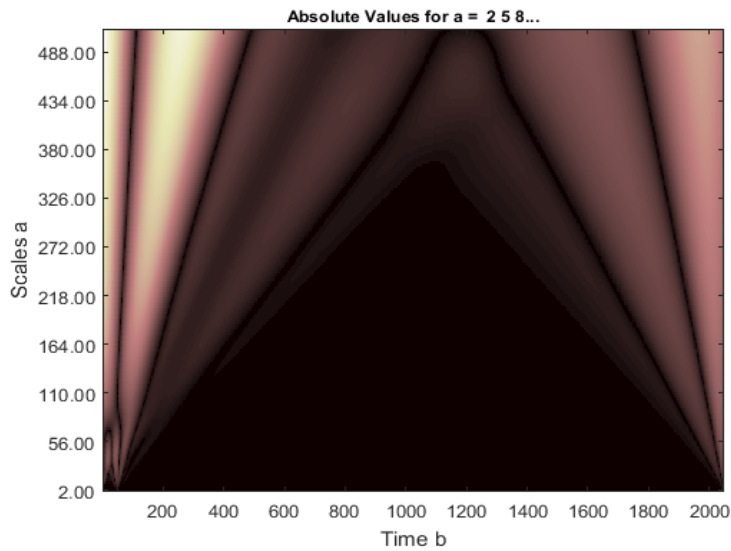


Fig. 2. Wavelet scalogram registered for test in which connection between the induction motor drive and the mechanical system loading him has been cut off until moment of backlash's taking.

Fig. 2 presents the wavelet scalogram depicting the linear acceleration of the induction motor drive a_1 with the inertia moment amounting to the value of true mass inertia moment J_1 decreased by about 7.5%. This simulation test has been conducted with backlash zone width = 0.005 at the consistency's coefficient $\eta_k = 0.025$ and the melt flow index $n_1 = 0.93$.

4. DESCRIPTION OF THE DIAGNOSTIC ALGORITHM USED IN PROCESSING OF THE WAVELET SCALOGRAMS BY MEANS OF IMAGE ANALYSIS METHOD WITH USING OF A CLUSTERING TECHNIQUE

According to the presented diagnostic procedure, the values of inertia moment J_1 with the assumed backlash zone width values of matrix X_3 are determined using normalization of values of matrix's elements X_2 .

For all the tested physical quantities, values of elements of matrix X_3 have been calculated as the transformation of the values X_2 to the range $[k_3, 2 \cdot k_3 - h_3]$ according to the formula:

$$X_{3(e)(a,b)} = \left(\frac{(X_{2(e)(a,b)} - h_2)}{k_2 - h_2} \right) \cdot (k_3 - h_3) + k_3; \quad (2)$$

$$a = 1, 2, \dots, 343; \quad b = 1, 2, \dots, 436; \quad e \in \langle 1, 6 \rangle$$

where: X_2 – values of matrix's elements calculated in the test,

h_2 – the minimal value of elements of matrix X_2 determined in the test,

k_2 – the maximal value of elements of matrix X_2 determined in the test,

h_3 – the initial value of the range containing normalized values X_2 in the test,

k_3 – the final value of the range containing normalised values X_2 in the test.

Therefore, the values of variables h_2 and k have been calculated according to the following formulas:

$$h_2 = \min(X_{2(e)(a,b)}); \quad a = 1, 2, \dots, 343; \quad b = 1, 2, \dots, 436; \quad e \in \langle 1, 6 \rangle \quad (3)$$

$$k_2 = \max(X_{2(e)(a,b)}); \quad a = 1, 2, \dots, 343; \quad b = 1, 2, \dots, 436; \quad e \in \langle 1, 6 \rangle \quad (4)$$

For all the tested physical quantities, values of elements of matrix X_2 have been calculated as the transformation of pixel colour intensities comprised in matrix X_1 to the range $[k_3, 2 \cdot k_3 - h_3]$.

Normalization of values of the elements of the matrix X_1 used in simulation tests conducted at consistency coefficient $\eta_k = 0.025$ with the assumed backlash zone width can be described according to the formula:

$$X_{2(e)(a,b)} = \left(\frac{(X_{1(e)(a,b)} - h_1)}{k_1 - h_1} \right) \cdot (k_3 - h_3) + k_3; \quad a = 1, 2, \dots, 343; \quad b = 1, 2, \dots, 436; \quad e \in \langle 1, 6 \rangle \quad (5)$$

where: X_1 – values of the elements of the matrix recorded in the test conducted with the nominal value of inertia moment J_1 (in the case of the undamaged drive with the induction motor),

h_1 – the minimal value of the elements of the matrix X_1 determined in the test,

k_1 – the maximal value of the elements of the matrix X_1 determined in the test,

h_3 – the initial value of the range containing normalized values X_1 determined in the test in which one assumed consistency coefficient $\eta_k = 0.025$ and nominal value of inertia moment J_1 ,

k_3 – the end value of the range containing normalised values X_1 determined in the test in which one assumed consistency coefficient $\eta_k = 0.025$ and nominal value of inertia moment J_1 .

Calculations of values of variables h_1 and k_1 have been performed using the following formulas:

$$h_1 = \min(X_{1(e)(a,b)}); a = 1,2...343; b = 1,2...436; e \in \langle 1,6 \rangle \quad (6)$$

$$k_1 = \max(X_{1(e)(a,b)}); a = 1,2...343; b = 1,2...436; e \in \langle 1,6 \rangle \quad (7)$$

Values of variables h_3 and k_3 , which represent the beginning and end of the range to which the values of the elements of matrix X_2 have been transformed. For all the tested physical quantities, they have been determined using the minimal and maximal value, respectively, according to the formulas:

$$h_3 = \min(h_4, k_4) \quad (8)$$

$$k_3 = \max(h_4, k_4) \quad (9)$$

where: h_4, k_4 – values of variables obtained as a result of calculations conducted using variables calculated for parts of samples recorded in the test.

On the basis of results obtained in the series of tests, it was decided to divide of calculation of values of variables h_4 and k_4 into two cases for every simulation test conducted with the assumed backlash zone width:

- the first case concerns linear acceleration on the circuit of the drive wheel of the rotor a_1 and linear speed of the mass v_2 ,
- the second case concerns the electromagnetic moment of the induction motor m_{el} , angular speed of the rotor ω_1 and linear acceleration of the mass a_2 .

In the first case, values of variables h_4 and k_4 have been calculated according to the following formulas:

$$h_4 = \min(X_{1(e)(j)}) - \max(X_{1(e)(j)}); e \in \langle 1,6 \rangle; j = 1,2...2048; \quad (10)$$

$$k_4 = \min(X_{1(e)(j)}) + \max(X_{1(e)(j)}); e \in \langle 1,6 \rangle; j = 1,2 \dots 2048; \quad (11)$$

In the second case, calculations of differences between the minimal and maximal values of arithmetic means of appropriate parts of the samples chosen from the matrix N_1 have been applied. However, values of variables h_4 and k_4 have been calculated, respectively, according to the formulas:

$$h_4 = (m_{e2} - m_{d2}) + (m_{e2} - m_{d2}) + (m_{e3} - m_{d3}) \quad (12)$$

$$k_{d4} = (m_{e1} - m_{d1}) - (m_{e2} - m_{d2}) - (m_{e3} - m_{d3}) - (m_{e4} - m_{d4}) \quad (13)$$

The minimal values m_{e1} , m_{e2} , m_{e3} , and m_{e4} used to determine the values of variables h_4 and k_4 have been calculated by means of the following formulas:

$$m_{e1} = \min(N_{1(e)(j)}); e \in \langle 1,6 \rangle; j = 1,2 \dots 768; \quad (14)$$

$$m_{e2} = \min(N_{1(e)(j)}); e \in \langle 1,6 \rangle; j = 1,2 \dots 1024; \quad (15)$$

$$m_{e3} = \min(N_{1(e)(j)}); e \in \langle 1,6 \rangle; j = 1,2 \dots 1280; \quad (16)$$

$$m_{e4} = \min(N_{1(e)(j)}); e \in \langle 1,6 \rangle; j = 1,2 \dots 1536; \quad (17)$$

The values of arithmetic means m_{d1} , m_{d2} , m_{d3} and m_{d4} have been calculated in the following way:

$$m_{d1} = \frac{\sum_{j=1}^{768} N_{1(e)(j)}}{768}; e \in \langle 1,6 \rangle \quad (18)$$

$$m_{d2} = \frac{\sum_{j=1}^{1024} N_{1(e)(j)}}{1024}; e \in \langle 1,6 \rangle \quad (19)$$

$$m_{d3} = \frac{\sum_{j=1}^{1280} N_{1(e)(j)}}{1280}; e \in \langle 1,6 \rangle \quad (20)$$

$$m_{d4} = \frac{\sum_{j=1}^{1536} N_{1(e)(j)}}{1536}; e \in \langle 1,6 \rangle \quad (21)$$

Values of elements of matrix N_1 have been determined according to the following order:

$$N_{1(e)(j)} = [M_{(e)(1)} \succcurlyeq M_{(e)(2)} \succcurlyeq \dots \succcurlyeq M_{(e)(2048)}]; e \in \langle 1,6 \rangle; j = 1,2 \dots 2048 \quad (22)$$

where: M – values of the elements of matrix M recorded in the test.

In the presented diagnostic method, determining of values of pattern matrices used in the identification of inertia moment J_1 was essential. Calculations in the algorithm were conducted according to the clustering method using *k-harmonic means* technique (Frąckiewicz, 2011).

An important element of the diagnostic method was conducting the most profitable initialisation of preliminary values of centres of clusters, membership function and weight function.

The initial values of centres of clusters used in simulations have been calculated by means of the value of variable k_3 obtained as a result of simulations conducted with consistency coefficient $\eta_k = 0,025$ [Pa·s^{n₁}] during which the inertia moment J_1 was changed at the assumed backlash zone width.

In simulations conducted by means of the described method, values of inertia moments J_1 have been used and chosen in sequence and according to the order assumed in matrix K_1 .

Calculations of the initial values of centres of clusters S conducted according to the following formula:

$$S_{(e)(i)} = 1 - k_3; \quad e \in \langle 1,6 \rangle; i = 1,2 \dots 7 \quad (23)$$

where: k_3 – the value of the variable determined according to the formula (8) by means of values of the matrix elements X_1 in simulations conducted for all the assumed changes of inertia moment J_1 .

Values of membership function have been written in matrix M , whereas the values of weight function have been written in matrix W . The initial values in both matrices were set equal to 1 and determined in the following way:

$$M_{(i)(a,b)} = 1; \quad a = 1,2 \dots 343; b = 1,2 \dots 436; i = 1,2 \dots 7 \quad (24)$$

$$W_{(a,b)} = 1; \quad a = 1,2 \dots 343; b = 1,2 \dots 436 \quad (25)$$

In the next step of the algorithm, the above-described initial values of membership function M and weight function W have been changed using the following formulas (Frąckiewicz, 2011):

$$W_{(a,b)} = \frac{\sum_{i=1}^7 \|X_{3(e)(a,b)} - S_{(e)(i)}\|^{-p-2}}{\left(\sum_{i=1}^7 \|X_{3(e)(a,b)} - S_{(e)(i)}\|^{-p}\right)^2}; \quad (26)$$

$$a = 1,2...343; b = 1,2...436; e \in \langle 1,6 \rangle; p \geq 2$$

$$M_{(i)(a,b)} = \frac{\|X_{3(e)(a,b)} - S_{(e)(i)}\|^{-p-2}}{\sum_{i=1}^7 \|X_{3(e)(a,b)} - S_{(e)(i)}\|^{-p-2}}; \quad (27)$$

$$a = 1,2...343; b = 1,2...436; e \in \langle 1,6 \rangle; i = 1,2...7; p \geq 2$$

where: p – additional optimisation parameter.

In the applied diagnostic method, the “soft” values of the membership function M have been calculated and met the following conditions (Frąckiewicz, 2011):

$$0 \leq M_{(i)(a,b)} \leq 1; a = 1,2...343; b = 1,2...436; e \in \langle 1,6 \rangle; i = 1,2...7; p \geq 2 \quad (28)$$

$$\sum_{i=1}^7 M_{(i)(a,b)} = 1; \quad a = 1,2...343; b = 1,2...436; i = 1,2...7 \quad (29)$$

Changes in the values of the membership function and the weight function have a significant impact on the values of the centres of clusters. It is then followed by determining a degree of membership of every value of the element of matrix X_3 to the particular clusters.

After updating of the values of the membership function M and weight function W , new values of centres of clusters S have been determined by means of the following formula (Frąckiewicz, 2011):

$$S_{(e)(i)} = \frac{\sum_{a=1}^{343} \sum_{b=1}^{436} (M_{(i)(a,b)} \cdot W_{(e)(a,b)} \cdot X_{3(e)(a,b)})}{\sum_{a=1}^{343} \sum_{b=1}^{436} (M_{(i)(a,b)} \cdot W_{(e)(a,b)})}; \quad e \in \langle 1,6 \rangle; i = 1,2...7 \quad (30)$$

In the conducted simulation tests, creation of pattern matrices as well as tested matrices have been conducted at the same assumed backlash zone width for all the tested physical quantities.

Values of all the elements of each pattern matrix have been calculated in the series of simulation tests in which the assumed consistency coefficient $\eta_k = 0.025$.

These values have been written to 7x7 matrix N_2 . The tested values have been written into the 1x7 matrix N_3 .

Values of the matrix's elements S have been written to the matrix containing pattern values N_2 and to the tested matrix N_3 . Therefore, matrices N_2 and N_3 have been determined according to the following formulas:

$$N_{2(e)(f,i)} = S_{(e)(f,i)}; e \in \langle 1,6 \rangle; f = 1,2...7; i = 1,2...7 \quad (31)$$

$$N_{3(e)(i)} = S_{(e)(i)}; e \in \langle 1,6 \rangle; i = 1,2...7 \quad (32)$$

Determination of the values of the elements of matrix H enables one for correct identification of the value of inertia moment for the calculated wavelet scalogram of the physical quantity at the particular consistency coefficient η_k .

Values of matrix H can be expressed by means of the formula:

$$H_{(f)} = h_5 \cdot \sum_{i=1}^7 |N_{2(f,i)} - N_{3(i)}|; f = 1,2...7; i = 1,2...7 \quad (33)$$

where: h_5 – the value of the variable used to improve the identification results.

Using of variable's value h_5 in calculations of matrix H clearly improves the results of the fault identification. The value of this variable causes the increase in the value obtained as a result of the summation of absolute values of differences between the values of the matrix containing pattern values N_2 and values of the tested matrix N_3 .

The most profitable for identification simulations variable's value h_5 calculated for tests conducted with all set changes of value of inertia moment J_1 for assumed backlash zone width and in the group of analysis with the adopted consistency coefficient $\eta_k = 0.025$.

To calculate the variable's value h_5 the following formula is used:

$$h_5 = \frac{\max(S_{(e)(i)}, S_{1(e)(i)})}{\min(h_3, k_3)}; e \in \langle 1,6 \rangle; i \in \langle 1,7 \rangle \quad (34)$$

Calculations of values of matrix's elements S_l were conducted employing the same methodology as for calculations of values of matrix S . It can be described by the formula:

$$S_{1(e)(i)} = 1 - h_{d3}; e \in \langle 1,6 \rangle; i = 1,2...7 \quad (35)$$

where: h_3 – the value of a variable determined according to the formula (8) by means of values of elements of matrix X_1 for simulation tests conducted for all the assumed changes of values of inertia moment J_1 .

Index nr (for $nr \in \langle 1, 7 \rangle$) in matrix H determines the column number in the matrix K_1 , which contains the correct inertia moment of reduced masses on the shaft of induction motor drive. The value of index nr ($nr \in \langle 1, 7 \rangle$) for $i = 1, 2, \dots, 7$ in matrix H has been determined using the following minimum function: $H_{(nr)} = \min(H_{(i)})$. Therefore, the number i of a column in the matrix K_1 refers to the corresponding to it index nr ($i = nr$).

5. RESULTS OF SIMULATIONS OF THE DIAGNOSTIC ALGORITHM APPLIED FOR IDENTIFICATION OF INERTIA MOMENT OF REDUCED MASSES ON SHAFT OF INDUCTION MOTOR DRIVE IN ELECTROMECHANICAL SYSTEM

In the tables presented below, in the column named *Test Parameters*, backlash zone widths have been placed assumed in the process of identification of the value of inertia moment of reduced masses connected stiffly with the motor's rotor J_1 . Besides, in the following tables, one bolded the correct results that were obtained finally in the process of identification of fault and that are the final results of calculations of matrix H .

For all tested physical quantities, pattern matrices N_1 have been created in a series of tests in which the assumed value of consistency coefficient η_k was equal to 0.025 [$\text{Pa} \cdot \text{s}^{-n_1}$]. Pattern matrices N_1 have been created for analyses in which an additional optimisation parameter p has been adopted corresponding to the assumed value of this variable. This value has been placed in the tables presented below.

Tab. 1. Exemplified results of tests in matrix H for linear acceleration of the induction motor drive a_1

Test parameters	Results	Test parameters	Results
inertia moment $J_1 = 0.957$, backlash zone = 0.00375, $\eta_k = 0.0375$, optimisation parameter $p = 2$	9.5409 8.4485 7.3105 6.0374 0.0671 10.5406 11.4658	inertia moment $J_1 = 0.957$, backlash zone = 0.00375, $\eta_k = 0.0375$, optimisation parameter $p = 3$	9.4615 8.3730 7.2421 5.9764 0.0675 10.4579 11.3810
inertia moment $J_1 = 1.131$, backlash zone = 0.01, $\eta_k = 0.0375$, optimisation parameter $p = 3$	0.0115 0.0001 0.0128 0.0276 0.1080 0.0212 0.0297	inertia moment $J_1 = 1.131$, backlash zone = 0.01, $\eta_k = 0.0375$, optimisation parameter $p = 9$	0.0150 0.0002 0.0166 0.0357 0.1333 0.0276 0.0380

Tab. 2. Exemplified results of tests in matrix H for electromagnetic moment of the induction motor drive m_{el}

Test parameters	Results	Test parameters	Results
inertia moment $J_1 = 1.102$, backlash zone = 0.0075, $\eta_k = 0.0125$, optimisation parameter $p = 2$	0.7347 0.3730 0.0012 0.4137 2.4923 1.0490 1.3497	inertia moment $J_1 = 1.102$, backlash zone = 0.0075, $\eta_k = 0.0125$, optimisation parameter $p = 3$	1.0650 0.5381 0.0023 0.5904 3.4786 1.5264 1.9718
inertia moment $J_1 = 1.189$, backlash zone = 0.01, $\eta_k = 0.05$, optimisation parameter $p = 3$	0.4008 0.8187 1.3102 1.7962 4.2535 0.0050 0.3993	inertia moment $J_1 = 1.189$, backlash zone = 0.01, $\eta_k = 0.05$, optimisation parameter $p = 9$	0.3424 0.7000 1.1203 1.5364 3.6411 0.0046 0.3415

Tab. 3. Exemplified results of tests in matrix H for angular speed of the rotor of the induction motor drive ω_1

Test parameters	Results	Test parameters	Results
inertia moment $J_1 = 1.218$, backlash zone = 0.005, $\eta_k = 0.0125$, optimisation parameter $p = 2$	0.8648 1.3365 1.8056 2.3249 4.8432 0.4357 0.0604	inertia moment $J_1 = 1.218$, backlash zone = 0.005, $\eta_k = 0.0125$, optimisation parameter $p = 3$	0.8659 1.3383 1.8080 2.3280 4.8496 0.4363 0.0604
inertia moment $J_1 = 1.218$, backlash zone = 0.0025, $\eta_k = 0.05$, optimisation parameter $p = 3$	0.9500 1.6000 2.2706 2.9889 6.4174 0.3959 0.1762	inertia moment $J_1 = 1.218$, backlash zone = 0.0025, $\eta_k = 0.05$, optimisation parameter $p = 6$	0.9391 1.5815 2.2445 2.9548 6.3460 0.3913 0.1741

According to the results of presented simulation tests, obtaining of correct results of identification of fault for all the tested physical quantities is possible if optimisation parameter p is equal or bigger than 2.

Tab. 4. Exemplified results of tests in matrix H for linear speed of the mass v_2

Test parameters	Results	Test parameters	Results
inertia moment $J_1 = 1.218$, backlash zone = 0.01, $\eta_k = 0.0125$, optimisation parameter $p = 2$	1.7737 2.7766 3.8581 5.0250 10.7233 0.8414 0.0263	inertia moment $J_1 = 1.218$, backlash zone = 0.01, $\eta_k = 0.0125$, optimisation parameter $p = 3$	1.8340 2.8699 3.9862 5.1898 11.0535 0.8704 0.0272
inertia moment $J_1 = 1.073$, backlash zone = 0.009, $\eta_k = 0.0375$, optimisation parameter $p = 3$	3.3018 2.2717 1.1624 0.0330 5.8461 4.2600 5.1521	inertia moment $J_1 = 1.073$, backlash zone = 0.009, $\eta_k = 0.0375$, optimisation parameter $p = 6$	1.8634 1.2977 0.6724 0.0195 3.6275 2.3761 2.8415

One should pay attention to the fact that if the value of additional optimisation parameter p exceeds 3, it triggers noticeable differences in results of fault's identification. Such conclusions can be drawn from the minimal values of matrix H obtained for the calculated wavelet scalograms. It can be noticed in all the presented tables.

6. CONCLUSIONS

The presented system of damage detection – based on image analysis enabling for the determination of centres of clusters by means of using the changes of value of membership function and weight function – found its application in the identification of the value of the inertia moment of rotating masses connected stiffly with the induction motor's rotor. The identification process has been conducted in the assumed time ranges.

The use of image analysis greatly increases the efficiency of analysis of non-stationary signals. This method, used in a diagnostic system, can effectively reduce the consequences of appearing of faults because it can be successfully applied already in the initial phase of the development of a fault. The conducted simulation confirmed the functioning of the proposed methodology of fault detection.

On the basis of the conducted research, it can be stated that the efficiency of detection process and fault identification can be greatly enhanced through ensuring appropriate ranges of changes of parameters and through the transformation the colour intensity of pixels recorded at wavelet scalogram in a system containing non-zero backlash zone to adequate ranges.

REFERENCES

- Divdel, H., Moghaddam, M. H., & Alipour, G. (2016). A new diagnosis of severity broken rotor bar fault based modeling and image processing system. *Journal of Current Research in Science*, *S*(1), 771–780.
- Duda, J. T. (2007). *Pozyskiwanie wzorców diagnostycznych w komputerowych analizach sprawności urządzeń. Diagnostyka procesów i systemów*. Warsaw, Poland: Akademicka Oficyna Wydawnicza EXIT.
- Frąckiewicz, M. (2011). *Zastosowanie techniki KHM (k-średnich harmonicznych) w przetwarzaniu obrazów barwnych* (Unpublished doctoral dissertation). Silesian University of Technology, Gliwice.
- Głowacz, A., & Głowacz, Z. (2017). Diagnosis of the three-phase induction motor using thermal imaging. *Infrared & Physics Technology*, *81*, 7–16.
- Hasiewicz, Z., & Śliwiński, P. (2005). *Falki ortogonalne o zwartym nośniku*. Warsaw, Poland: Akademicka Oficyna Wydawnicza EXIT.
- Korbicz, J., Kościelny, J. M., & Kowalczyk, Z. (2002). *Diagnostyka procesów. Modele. Metody sztucznej inteligencji. Zastosowania*. Warsaw, Poland: WNT.
- Looney, C. G. (1997). *Pattern recognition using neural networks*. New York, USA: Oxford University Press.

- Mathew, G. (2017). Fault detection in an induction motor drive using discrete wavelet packet transform. *IOSR Journal of Electrical and Electronics Engineering (IOSR-JEEE)*, 12(2), 01–06.
- Wolkiewicz, M., & Kowalski, Cz. (2015). Diagnostyka uszkodzeń uzwojeń stojana silnika indukcyjnego z wykorzystaniem dyskretnej transformaty falkowej obwiedni prądu stojana. *Maszyny elektryczne: zeszyty problemowe*, 3(107), 13–18.
- Wysocki, H. (2006). *Zastosowanie nieklasycznego rachunku operatorów do identyfikacji liniowych układów dynamicznych*. Warsaw, Poland: Akademicka Oficyna Wydawnicza EXIT.
- Zajac, M. (2009). *Metody falkowe w monitoringu i diagnostyce układów elektromechanicznych (No. 371)*. Cracow, Poland: Politechnika Krakowska.
- Sajjad, S., Zaidi, H., Zanardelli, W. G., Aviyente, S., & Strangas, E. G. (2007). Comparative study of time-frequency methods for the detection and categorization of intermittent faults in electrical drives. In *Proc. IEEE Int. Symp. on Diagnostics for Electrical Machines, Power Electronics and Drives* (pp. 39–45). Cracow.